frontiers in Built Environment

TYPE Original Research
PUBLISHED 28 April 2026
DOI 10.3389/fbuil.2026.1824451

Check for updates

OPEN ACCESS

EDITED BY
Fabrizio Mollaioli,
Sapienza University of Rome, Italy

REVIEWED BY
Rodolfo Labernarda,
University of Calabria, Italy
Khelaifia Akram,
University of Biskra, Algeria

*CORRESPONDENCE
Amirhossein Ghezelbash,
a.ghezelbash@tudelft.nl

RECEIVED 06 March 2026
REVISED 23 March 2026
ACCEPTED 24 March 2026
PUBLISHED 28 April 2026

CITATION
Ghezelbash A, Rots JG and Messali F (2026) Numerical study of the effects of tilting base on seismic out-of-plane response of one-way spanning unreinforced masonry walls.
Front. Built Environ. 12:1824451.
doi: 10.3389/fbuil.2026.1824451

COPYRIGHT
© 2026 Ghezelbash, Rots and Messali. This is an open-access article distributed under the terms of the Creative Commons Attribution License (CC BY). The use, distribution or reproduction in other forums is permitted, provided the original author(s) and the copyright owner(s) are credited and that the original publication in this journal is cited, in accordance with accepted academic practice. No use, distribution or reproduction is permitted which does not comply with these terms.

Numerical study of the effects of tilting base on seismic out-of-plane response of one-way spanning unreinforced masonry walls

Amirhossein Ghezelbash*, Jan G. Rots and Francesco Messali

Faculty of Civil Engineering and Geosciences, Delft University of Technology, Delft, South Holland, Netherlands

This paper investigates the response of one-way spanning unreinforced masonry (URM) walls first statically tilted in the in-plane (IP) and out-of-plane (OOP) directions and then subjected to seismic OOP loading, a subject largely overlooked in the literature. The study is motivated by this knowledge gap and its particular relevance to Netherlands, where ground settlement often leads to visible tilting in buildings, yet sufficient evidence for if and how such tilting should be explicitly considered in design and assessment does not exist. The numerical modeling approach previously proposed by the authors, validated against complex experimental data, is employed in a comprehensive parametric study to provide preliminary insights into the seismic response of tilted walls. The model represents URM unit-by-unit using nonlinear 3D solid expanded blocks and cohesive-frictional zero-thickness joints. Two wall specimens, one short and one long, are subjected to one level of IP base tilting and two levels of OOP base tilting. Static and dynamic OOP loading is then applied while maintaining the prescribed tilt. Under static OOP loading, three levels of vertical pre-compression are considered, representing conditions in low-rise residential buildings. For dynamic OOP analyses, a multi-step loading sequence with varying levels of overburden is used. The results show negligible sensitivity to IP tilting (even up to 4°). While the specimens exhibit slightly greater sensitivity to OOP tilting, primarily due to reduced vertical confinement and increased uplift, responses remain largely stable even with large OOP drift (up to 22% of wall thickness). Aside from the aforementioned findings, this study, being the first one in the literature studying load-bearing tilted walls, highlights key limitations which may have affected the outcomes and emphasizes the need for further research to better understand the behavior of tilted URM walls.

KEYWORDS
base rotation, numerical modeling, out-of-plane, seismic loading, tilt, unreinforced masonry

1 Introduction

Unreinforced masonry (URM) is one of the oldest structural materials and constitutes a substantial portion of the existing low-to mid-rise building stock worldwide, and representing a significant share of residential buildings particularly in Europe (Koc et al., 2023). Such wide usage reflects the long-standing economic and practical appeal of URM due to the availability of local materials, good vertical load-bearing capacity,

thermal and acoustic insulation, and fire resistance (Page, 1995). However, a large fraction of this global URM stock predates modern seismic codes and has not been designed for earthquake resistance, making seismic safety a major concern in many regions (Parisi and Augenti, 2013). Extensive post-earthquake observations and several comprehensive reviews have shown that URM buildings are especially vulnerable to earthquake loading perpendicular to the plane of their walls, referred to as out-of-plane (OOP) loading, with the OOP failure of wall panels, parapets, and gables often causing structural collapse and life-safety risk (Canditone et al., 2025). Among the various OOP responses, one-way spanning walls are particularly vulnerable. One-way OOP bending mechanisms, observed in walls restrained only at two parallel edges, are typically governed by rocking and sliding equilibrium at mortar joints rather than the strength of the URM units. As such, they can be triggered by relatively modest horizontal accelerations once cracks or separations develop at wall supports or between wall segments (Al Shawa et al., 2012). Numerous experimental and analytical studies have therefore focused on the dynamic OOP response of one-way (or vertically spanning) URM walls (Derakhshan et al., 2016; Penner and Elwood, 2016b; 2016a).

In certain regions of the world, such as Netherlands, OOP failure in low-rise URM buildings is a particular concern. Because of the historical low seismicity of the country (van Ginkel et al., 2022), the URM walls used in construction are typically designed with high slenderness, that is, large heights and low thicknesses, a combination that increases vulnerability to OOP loads (Galanakis, 2019). This vulnerability is further intensified by the geotechnical conditions of the region, as large parts of the country are founded on soft Holocene Peats and Clays, which are highly compressible and prone to long-term subsidence and differential settlement (Korswagen et al., 2024; Prosperi et al., 2024; Prosperi, 2025). Many URM buildings in Dutch towns, such as those in the Groningen province, rest on shallow or ageing pile foundations in these soft soils and have been documented to experience long-term visible deformation, referred to as tilting, due to settlement (Peduto et al., 2016; 2019; Nicodemo et al., 2020). Several studies have developed fragility and consequence models for settlement-affected masonry buildings, highlighting that permanent rotations caused by settlement can significantly alter structural demand and capacity (Peduto et al., 2017; 2019; Prosperi et al., 2023a). However, current assessment approaches do not account for the effects of such pre-existing base tilting on the seismic response of URM buildings (Crowley et al., 2017; Galanakis, 2019). Likewise, existing design and assessment guidelines include no provisions regarding base tilting effects (Canadian Standards Association, 2004; European Committee for Standardization, 2004; Standards New Zealand, 2004; ASCE 41-17: Seismic Evaluation and Retrofit of Existing Buildings, 2017; Netherlands Standardization Institute, 2020). In parallel, although retrofit solutions for existing URM walls can be effective, recent studies, such as (Labernarda and Mazza, 2026) have highlighted practical concerns related to their long-term durability, environmental degradation, wall geometry, and opening configuration. Therefore, further understanding is needed to develop more robust risk mitigation strategies.

This knowledge gap is further exacerbated by the lack of research on tilted URM walls and buildings in the literature. Numerous studies, including shake-table tests on one-way spanning walls, *in-situ* tests on vertically spanning strips, and numerical investigations, have been conducted on one-way spanning walls (Ferreira et al., 2015; Graziotti et al., 2016; Penner and Elwood, 2016b). However, none of these studies investigate configurations where the walls are initially tilted, either in-plane (IP) or OOP. Recently, two separate campaigns reported in (Al Shawa et al., 2012; Choi et al., 2023a; 2023b; Park et al., 2025) have explored the effects of tilting on the dynamic response of URM walls. While these studies provide valuable insights, they face notable limitations. The campaign in (Choi et al., 2023a; 2023b; Park et al., 2025), which investigates leaning URM fence walls through shake-table testing and numerical simulation, focuses on non-loadbearing configurations with different boundary conditions and mass distributions that differ substantially from those of one-way spanning loadbearing walls in buildings. Meanwhile, the study in (Al Shawa et al., 2012) examines the effects of OOP base tilting on a single rigid rocking block rather than a typical URM wall.

The scarcity of experimental data on IP- or OOP-tilted walls largely stems from the practical challenges of replicating realistic base tilting in laboratory or shake-table setups while simultaneously applying gravity and dynamic loads. Creating a controlled permanent tilt in the support system requires complex test rigs and may introduce unintended interactions between the specimen and the loading frame (Damiani et al., 2025). Moreover, most numerical studies either idealize the base as rigid and horizontal, neglecting base tilting effects, or simulate settlement-induced damage by applying settlement profiles at the wall base (Prosperi et al., 2023c; 2023b). While these approaches may be appropriate for two-way spanning walls, where long lengths and perpendicular elements lead to complex responses under settlement, such approaches tend to overcomplicate the modeling of the behavior of simpler configurations as explained in the following. One-way spanning URM walls, often constructed with relatively short lengths compared to the characteristic width of settlement troughs, tend to exhibit predominantly rigid-body settlement or tilt with limited angular distortion. This substantially reduces internal bending strains and cracking compared to longer, two-way spanning walls subjected to the same ground curvature (Charles and Skinner, 2004; Prosperi et al., 2023b; Kolivand and Daraei, 2024). Hence, an alternative, more representative approach is required for the numerical study of tilted one-way spanning walls.

The study presented in this paper contributes to addressing the abovementioned knowledge gap by conducting a comprehensive parametric study of how base tilting influences the response of one-way spanning load-bearing URM walls in typical low-rise buildings. In particular, the numerical approach proposed in (Ghezelbash et al., 2025b) for the high-fidelity dynamic simulation of seismic response of one-way spanning URM walls is employed to complement physical testing and generate new data that are otherwise difficult to obtain through experiments. In the modeling approach, URM is represented unit-by-unit with 3D nonlinear expanded solid blocks and cohesive frictional zero-thickness joints. The approach is preferred over simpler macro-element (Vanin et al., 2020; Malomo and DeJong, 2022; Kesavan and Menon, 2023; Guettala et al., 2025a) approaches as it does not enforce pre-defined failure paths, and also over continuum-based (Selby and Vecchio, 1993; Lourenço, 2000; Noor-E-Khuda et al., 2016; Rots et al., 2016; Noor-E-Khuda, 2021) models because it

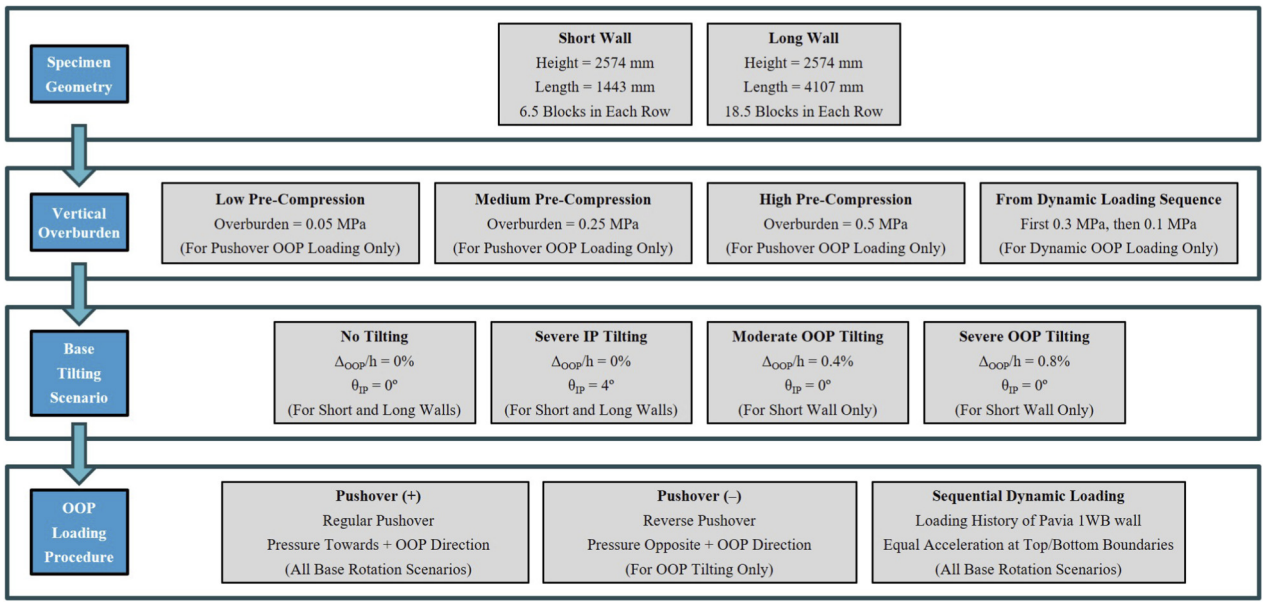


FIGURE 1
Overview of the parametric study procedure.

allows explicit simulation of cracking and collapse. Moreover, the approach is successfully used previously for the prediction and assessment of complex OOP responses (Ghezelbash et al., 2025d; 2025a; 2026), yielding reliable outcomes that conform with real-world responses. The paper is structured as follows. Section 2 presents the methodology adopted in this study, including the considered geometries, levels of vertical overburden, types and levels of base tilting, and OOP loading. As this investigation is intended to provide preliminary insights into the topic, a critical discussion of the adopted methodological limitations is also included, aiming to highlight areas for future improvement. Section 3 presents the results of the numerical simulations, which are then critically discussed and cross-compared with existing knowledge in Section 4. Specifically, the impact of base tilting on OOP stiffness, strength, deformation demands, and failure mechanisms during one-way OOP bending is discussed. The main outcomes of the study are ultimately presented in Section 5 with suggestions for future research.

2 Parametric study methodology

A numerical parametric study is conducted to investigate the effects of base tilting on the seismic response of URM walls, following the setup illustrated in Figure 1. In summary, two wall geometries are selected and subjected to pushover and dynamic one-way bending OOP loading under varying levels of base IP and OOP rotation; specifically, one level of IP base tilting and two levels of OOP base tilting. For the specimens subjected to subsequent pushover loading, different levels of pre-compression are also considered. The numerical model developed in (Ghezelbash et al., 2025b), originally created for a wall specimen tested under sequential one-way bending OOP dynamic loading at EUCENTRE (Pavia, Italy) (Graziotti et al., 2016), serves as the foundation for this parametric study. The additional variations described above are generated based on this model and calibrated to real-world structural conditions of low-rise residential URM buildings in Groningen province of Netherlands (Jafari et al., 2019). The following sections provide a more detailed explanation of the overall procedure.

It should be noted that the reliability and limitations of the modeling approach adopted in this study, including its numerical stability and sensitivity to damping and discretization, have been extensively investigated and reported in the previous studies of the authors (Ghezelbash et al., 2025b; 2025c; 2026). Although brief introductions to different aspects of the modeling approach are provided in the following sections, such sensitivity analyses are not repeated here for the sake of conciseness. Interested readers are therefore referred to the cited publications for further information. In particular (Ghezelbash et al., 2025b), provides additional detail on the numerical modeling choices to which affect the behavior of one-way spanning specimens simulated in this study.

2.1 Specimen geometries

As shown in Figure 2, two wall geometries are considered: one with a shorter length (referred to as the Short wall) and the other with a longer length (referred to as the Long wall). The Short wall has the same dimensions as the one-way bending numerical specimen developed in (Ghezelbash et al., 2025b) based on the benchmark experiment of EUCENTRE (Graziotti et al., 2016), with a length of 1443 mm, thickness of 102 mm, and height of 2754 mm. The Long wall adopts a geometry similar to the double-clamped COMP-4 wall tested in an experimental campaign at TU Delft (Netherlands) under quasi-static cyclic IP loading (Messali et al., 2020) and simulated in previous works of the authors (Ghezelbash et al., 2023b; 2023a),

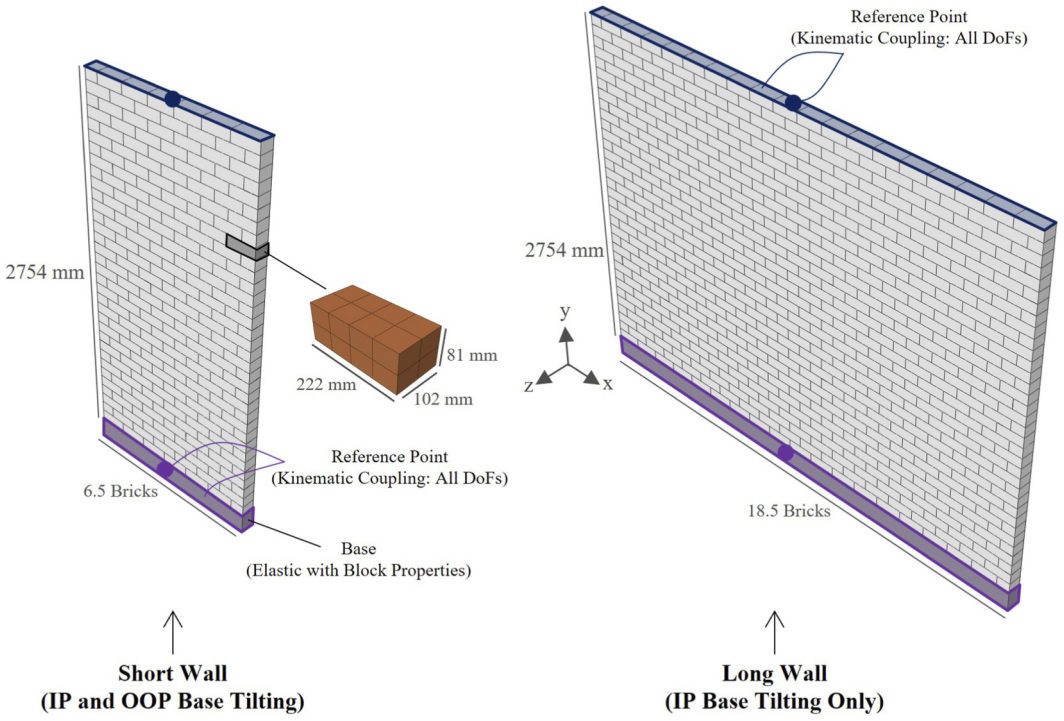


FIGURE 2
Geometry of the numerical wall specimens used in the parametric study.

sharing the same height and thickness as the Short wall but with an extended length of 4107 mm. While the Short wall is used to study OOP response under both IP and OOP base tilting scenarios, the Long wall is only considered under IP tilting. This allows investigation into whether a larger cross-section and/or greater mass influences the effect of base inclination. The omission of the Long wall from OOP tilting simulations is based on the expectation that both geometries would exhibit similar behavior under the one-way bending OOP loading scenario considered (see (Ghezelbash et al., 2025d; 2025b) for further explanation).

2.2 Mechanical characterization

The wall geometries are represented unit-by-unit via 222 × 81 × 102 mm^3 (length × height × thickness) expanded blocks in running bond configuration and zero-thickness joints, consistent with how the reference EUCENTRE experiment has been simulated in the previous work of the authors (Ghezelbash et al., 2025b). A visual summary of the modeling approach is shown Figure 3, demonstrating the finite-element discretization of the expanded blocks, the constitutive mechanical behaviors of the blocks and the joints, and the input parameters defining the constitutive behaviors. The input values for the mechanical parameters are the same as those used in the simulation of the benchmark experiment in (Ghezelbash et al., 2025b). These parameters are listed in Table 1 for ease of reference, while a detailed description of the constitutive material behaviors, as well as the calibration procedure for the input parameters is omitted here for brevity. Readers seeking more information are therefore referred to (Ghezelbash et al., 2025b). It should be noted that the adopted parameters correspond to typical Calcium Silicate brick masonry materials representative of the URM building stock in the Groningen province of Netherlands (Jafari et al., 2019).

2.3 Application of vertical overburden

For the dynamic analyses conducted in this study, the vertical loading procedure from the reference experiment (Graziotti et al., 2016) is adopted, as further detailed in Section 2.5 and in (Ghezelbash et al., 2025b). However, for specimens subjected to pushover analysis, three levels of vertical pre-compression, within the practical range typical of URM buildings in Netherlands (Messali et al., 2020), are considered to examine the influence of wall position within a building on its OOP response. These pre-compression levels are set at 0.1 MPa (LPC), 0.25 MPa (MPC), and 0.50 MPa (HPC), representing low, moderate, and high vertical overburden, respectively. The LPC scenario represents a lightly loaded wall in a single-story, as well as a wall on the second floor of a two-story building, supporting only a roof. The MPC condition simulates a ground-level wall in a two-story building, while the HPC case serves as an extreme scenario intended to activate compressive damage and highlight its effect on the OOP response. The vertical loads are applied as concentrated downward point forces at the top reference point of the walls, with magnitudes calculated by multiplying the intended pre-compression by the cross-sectional area of each wall geometry. These forces are kept vertical throughout the analysis to amplify second-order effects induced by base rotation. Such a setup also reflects the real-world conditions of the walls, wherein regardless of the orientation of the wall, the vertical load imposed by the top floors or roof remains downward. It should

10.3389/fbuil.2026.1824451

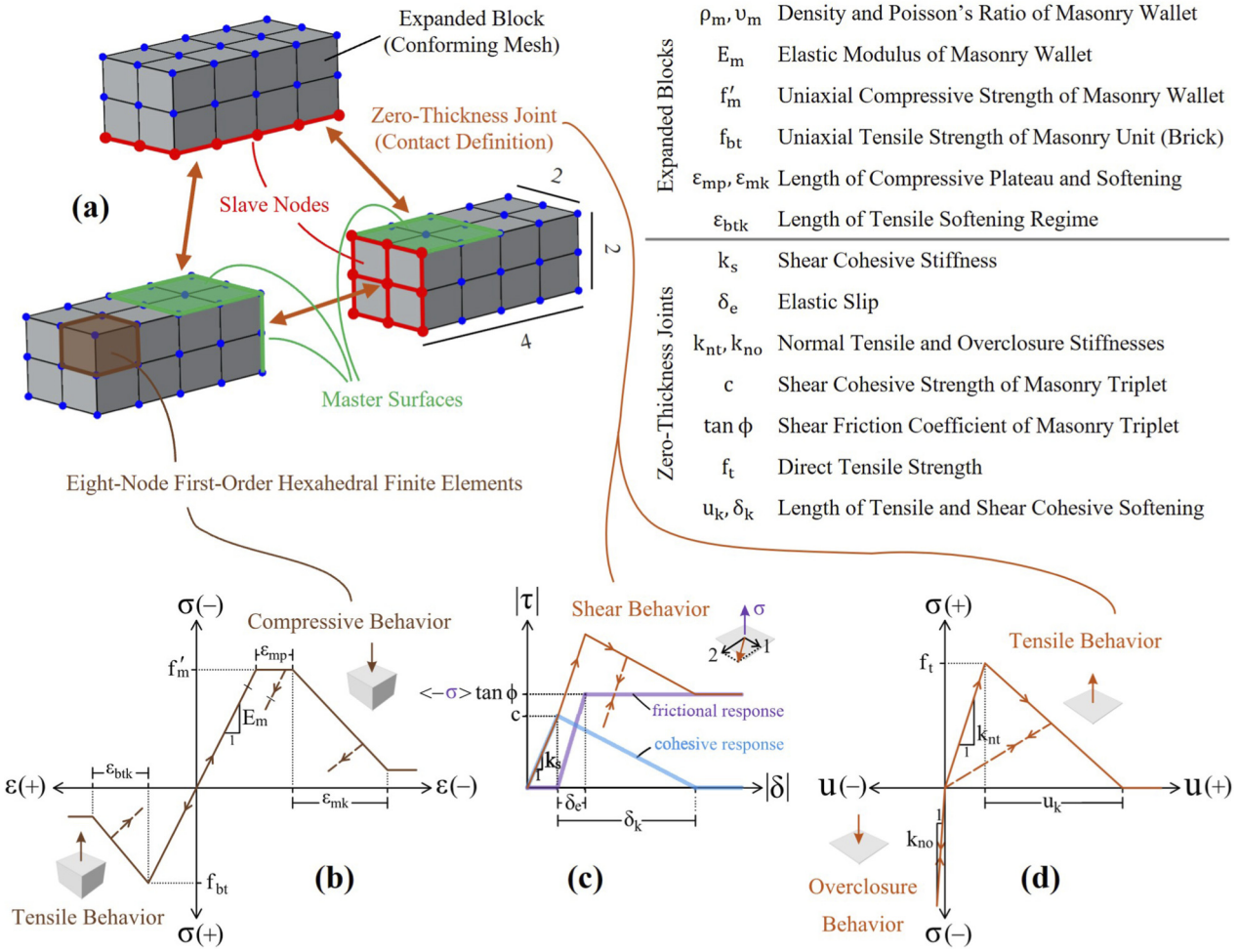


FIGURE 3
High-fidelity numerical modeling approach used in the parametric study of tilted walls: geometrical representation of URM **(a)**, compressive and tensile behavior of expanded blocks **(b)**, tangential shear response of the zero-thickness joints **(c)**, and their normal tensile and overclosure responses **(d)**. The shear response of the joints is drawn for a scenario where $<-\sigma>\tan\phi$ is larger than **(c)**, and elastic slip is steeper than cohesive stiffness.

TABLE 1 **Mechanical characterization inputs of the numerical models.**

Expanded Blocks							
Elastic behavior		CDP parameters		Compressive behavior		Tensile behavior	
E_m [MPa]	3236	ψ [°]	10	f'_m [MPa]	6.3	f_{bt} [MPa]	1.5
ν_m [−]	0.17	ϵ [−]	0.1	ε_{mp} [−]	0.006	ε_{btk} [−]	0.002
ρ_m [kg/m^3]	1852	f_{b0}/f_{c0} [−]	1.16	ε_{mk} [−]	0.010		
		ρ [−]	2/3				
Zero-thickness joints							
Overclosure behavior		Tensile cohesive behavior		Shear cohesive behavior		Shear frictional behavior	
k_{no} [N/mm^3]	241	k_{nt} [N/mm^3]	241	k_s [N/mm^3]	103	tan ϕ [−]	0.42
		f_t [MPa]	0.16	c [MPa]	0.21	δ_e [mm]	0.001
		u_k [mm]	0.4	δ_k [mm]	0.4		

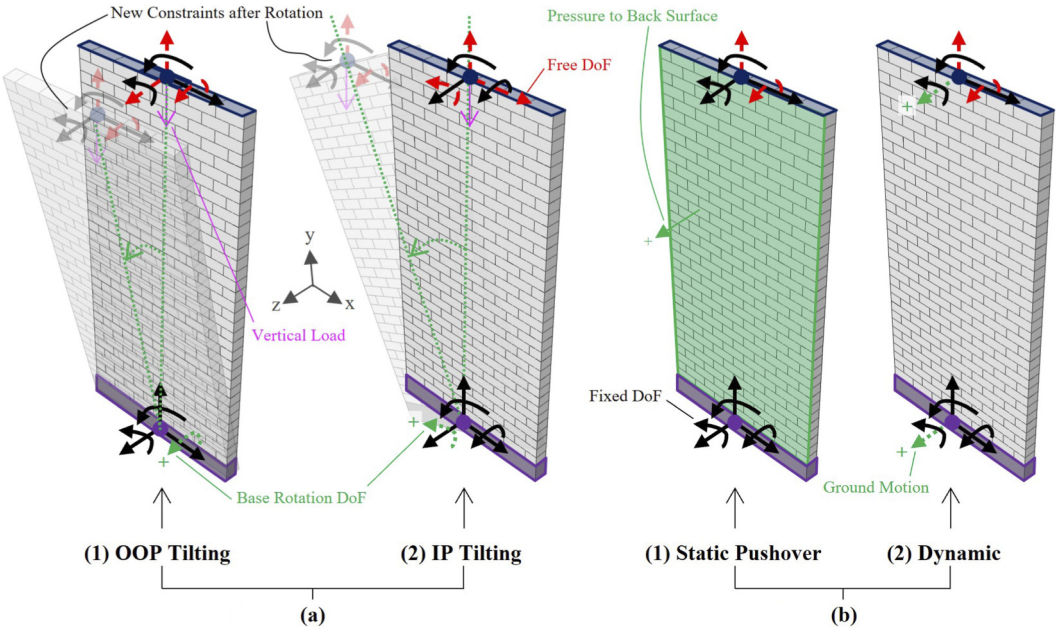


FIGURE 4
Boundary conditions during base tilting and OOP loading steps. **(a)** Base Tilting. **(b)** OOP Loading.

be noted that prior to the application of vertical overburden, all specimens are subjected to gravity (9.81 m/s^2). In the simulation, gravity and vertical overburden are each applied in a separate static analysis step, monotonically increasing to their prescribed values (see (Ghezelbash et al., 2025b) for more details).

2.4 Application of base tilting

Prior to the application of gravity, overburden, or base tilting, kinematic coupling is introduced to simplify the wall boundaries and facilitate the application of subsequent loads and constraints. Similar to the original numerical model of the authors (Ghezelbash et al., 2025b), the top surface of each wall is kinematically coupled to a reference point at its center of geometry. Moreover, the base is coupled to a reference point at its center of mass. Kinematic coupling constrains the coupled region to behave as a rigid body, with motion compatible with the nodal deformations of the reference point to which it is coupled.

For the walls considered for static OOP analysis, a new loading step is introduced after the application of gravity and vertical loading and prior to OOP loading to implement base tilting. In this step, the wall base is rotated in the IP or OOP plane by a prescribed amount. This step is analyzed using the static solver adopted for the gravity and vertical loading phases, as described in (Ghezelbash et al., 2025b). The boundary conditions used during the rotation step are illustrated in Figure 4a. During base tilting, all degrees of freedom (DoFs) at the base are constrained except the one corresponding to the prescribed rotation. At the top reference point, all DoFs are fixed except those necessary to accommodate the correct wall deformation during base tilting. Specifically, during IP base tilting, where the wall deforms IP and rotates about the OOP (z-axis), the x- and y-axis translations and z-axis rotation of the top reference point are released (Figure 4a.1). During OOP base tilting, where the wall deforms OOP and rotates about the IP (x-axis), the y- and z-axis translations, as well as the x-axis rotation, are released (Figure 4a.2). The rotation angles are directly applied to the base reference point, causing the entire base to undergo a rigid-body rotation by the prescribed amount. The cantilever boundary conditions of the wall ensure minimal artificial resistance during this process. For the walls considered for dynamic OOP analysis, a more complex base tilting procedure is used (with the change of vertical load after in-between OOP loading) which is explained later in Section 2.5.

For all walls under static or dynamic OOP analysis, one level of IP rotation and two levels of OOP rotation are considered. Due to the lack of specific field observations regarding the amount of tilt in low-rise residential URM buildings (Peduto et al., 2016; 2019; Nicodemo et al., 2020), the values of IP and OOP base tilting for the current study are adapted from other well-known real-world structures and numerical stability analyses, respectively. For IP base tilting, a relatively large rotation angle (θ_{IP}) of 4° is adopted, based on the documented tilting observed in the Garisenda Tower in Bologna (Italy) (Pesci et al., 2024) and the Leaning Tower of Pisa (Italy) (Burland et al., 2009). Although other existing URM towers exhibit even larger tilting, such as the medieval bell tower in Gau-Weinheim (Germany), which leans at 5.43° (RLP Tourismus website, 2025), the Italian towers are selected due to the higher seismic hazard in their locations. Both Bologna and Pisa are situated in one of most earthquake-prone regions of Europe, along the Apennine belt, which has a significantly higher seismic hazard and a more extensive history of damaging earthquakes compared to western Germany, including the Rhineland-Palatinate region where Gau-Weinheim is located (Danciu et al., 2021; 2024; Cito et al., 2022). As a result, despite its greater inclination, the Gau-Weinheim tower is not expected to be exposed to seismic actions as severe as those affecting the Italian towers, making its use as a benchmark

potentially overconservative. Since the 4° tilt represents the highest real-world inclination observed in URM structures located in seismically active regions, it is adopted as a representative "severe" IP tilting condition. It should be noted that the Tower of Pisa, from which the in-plane (IP) tilting magnitude is derived, has geometric and material properties that differ from those of the wall specimens studied here. Nevertheless, the current approach remains valid, as it offers insight into worst-case structural conditions.

For OOP base tilting, the rotation angles are selected based on the stability of the specimens under different levels of vertical overburden. Specifically, each of the three walls with low (0.1 MPa), moderate (0.25 MPa), and high (0.5 MPa) pre-compression is subjected to monotonically increasing OOP base tilting, and the highest angle that maintains stability across all three cases under subsequent OOP loading is adopted as the upper bound for the parametric study. This analysis revealed that the highly pre-compressed specimen exhibits the lowest OOP rotation capacity due to amplified second-order effects. In this case, a rotation angle of 0.5° leads to cantilever overturning. To ensure conservativeness and avoid stability issues during subsequent OOP loading, a maximum rotation angle of 0.46° is used as the larger OOP base tilt in the study, and half of this value is adopted as the second, smaller tilt. For engineering clarity, OOP base tilting is hereafter reported in terms of OOP drift, defined as the horizontal OOP displacement of the top reference point normalized by the wall height (Δ_{OOP}/h). The smaller and larger tilt angles correspond to OOP drifts of 0.4% and 0.8%, respectively. Although these tilts are significantly smaller than the one used for IP base tilting, they entail more severe consequences for the slender walls considered here. For example, the larger OOP tilt results in a top displacement equivalent to 22% of the wall thickness, which, as shown in previous works of the authors (Ghezelbash et al., 2025b; 2025c; 2025a) and in (Ministero delle Infrastrutture e dei Trasporti, 2008; Ministero delle Infrastrutture e dei Trasporti, 2018; University of Auckland, 2011), is close to the displacement threshold (25% of thickness) marking the onset of OOP instability and potential collapse free top boundaries (such as parapets). Thus, this magnitude is taken to represent a "severe" OOP rotation condition. The smaller tilt, corresponding to a displacement equal to 11% of the wall thickness, aligns with the initiation of cracking and the transition into a post-elastic response phase during one-way OOP bending, and is therefore associated with a "moderate" OOP base tilting condition.

A comparison between the tilt angles considered in this study and those reported in the literature shows that the severe OOP tilting angle (0.5°) considered here is consistent with values (Charles and Skinner, 2004) observed in excessively tilted low-rise buildings (0.57°). In contrast, the 4° IP tilt angle substantially exceeds the severe tilting values reported (Namazi and Mohamad, 2013) for real residential buildings (1.15°). Accordingly, while the OOP tilting analyses are expected to reasonably represent conditions relevant to real walls, the IP tilting analyses should be regarded as illustrative of extreme scenarios.

After base tilting, the top and bottom boundary conditions are updated to prepare the specimens for OOP loading. Specifically, all DoFs of the base reference point are fixed, and at the top reference point, only vertical uplift and rotation about the IP axis are kept free. It should be noted again that during base tilting, the vertical overburden is consistently applied in the downward direction. The implemented base tilting scenarios, combined with the geometrical and overburden variations introduced in previous sections, results in 18 rotated and 6 non-rotated wall configurations for pushover analysis, and 7 rotated and non-rotated configurations for dynamic analysis.

2.5 Application of OOP loading

After the application of IP or OOP base tilting, the walls are subjected to OOP loading. Two sets of OOP loading procedures are considered. The first includes static pushover applied to all specimens, and the second involves sequential dynamic loading applied only to selected variations. The boundary conditions and loading procedures for both pushover and dynamic OOP analyses are illustrated in Figure 4b. During pushover loading, all DoFs at the base and top reference points are fixed at their final positions from the preceding base tilting step, except for vertical uplift and x-axis rotation at the top reference point. This configuration mimics a flexible floor diaphragm, consistent with the boundary conditions adopted in the numerical model developed by the authors in (Ghezelbash et al., 2025b) to simulate the reference EUCENTRE experiment (Graziotti et al., 2016). This free-uplift, free-rotation, flexible-floor condition is especially appropriate, as it represents the scenario with the lowest OOP resistance among typical boundary configurations (see (Ghezelbash et al., 2025d) for further details). Pushover analysis is performed using the same static solver as that used for the base tilting step and involves applying a uniformly increasing pressure on the wall surface (Figure 4b.1). Walls under IP base tilting are subjected to pushover only in the positive z-direction, whereas those under OOP base tilting are also pushed in the negative z-direction to examine the directional influence of OOP base tilt on wall resistance. It should be noted that the OOP pressure is always applied perpendicular to the surface of the walls. In total, 24 pushover analyses are conducted, covering the various base tilting conditions and levels of vertical overburden explained in the previous section.

Dynamic analyses are performed for 7 wall configurations with varying levels of base tilting, using the original loading sequence from the benchmark EUCENTRE experiment (Graziotti et al., 2016), as previously adopted in the simulations in (Ghezelbash et al., 2025b). This sequence, detailed in Table 2, begins with gravity loading, followed by the application of 0.3 MPa pre-compression (as a downward concentrated force) at the top reference point, a sequence of dynamic loading steps (referred to as runs) with increasing intensity, a reduction in pre-compression to 0.1 MPa, and a second sequence of dynamic runs. The dynamic simulations are performed using the HHT-α implicit-based solution procedure, explained in detail in (Ghezelbash et al., 2025b), with the same solver and damping settings employed for the simulation of the reference one-way bending experimental wall. Damping calibration (5% Rayleigh damping over the frequencies of the first and second OOP deformation modes) is maintained unchanged across all wall configurations, as preliminary modal analysis, as well as the study in (Ghezelbash et al., 2025b), confirmed that wall length does not affect the natural frequencies associated with OOP deformation modes. For walls subjected to dynamic loading, base tilting is introduced through a new loading

TABLE 2 Loading sequence adopted in the dynamic simulations, adapted from (Graziotti et al., 2016).

0.3 MPa vertical compression applied				Vertical compression reduced to 0.1 MPa			
Run #	Input	Scale	PGA[i] [g]	Run #	Input	Scale	PGA [g]
0–1	WN	–	–	0–2	WN	–	–
1	Gr-1	20%	+0.04	14	Gr-1	40%	+0.08
2	Gr-1	40%	+0.09	15	Gr-1	80%	+0.17
3	Gr-1	80%	+0.16	16	Gr-1	100%	+0.21
4	Gr-1	100%	+0.20	17	Gr-1	160%	+0.34
5	Gr-1	160%	+0.32	18	Gr-1	200%	+0.41
6	Gr-1	200%	+0.42	19	Gr-1	250%	+0.51
7	Gr-1	250%	+0.52	20	Gr-1	300%	+0.60
8	Gr-1	350%	+0.74	21	Gr-1	350%	+0.73
9	Gr-1	450%	+0.96	22	RWA	100%	−0.26
10	RWA	400%	−1.11	23	RWA	200%	−0.48
11	RWA	600%	−1.63	24	RWA	300%	−0.72
12	RWA	400%	−1.05	25	RWA	300%	−0.96
13	RWA	600%	−1.88	26	Gr-2	100%	+0.44
				27	Gr-2	150%	+0.64
				28	Gr-2	200%	+0.85

[i]Recorded Peak Ground Acceleration.

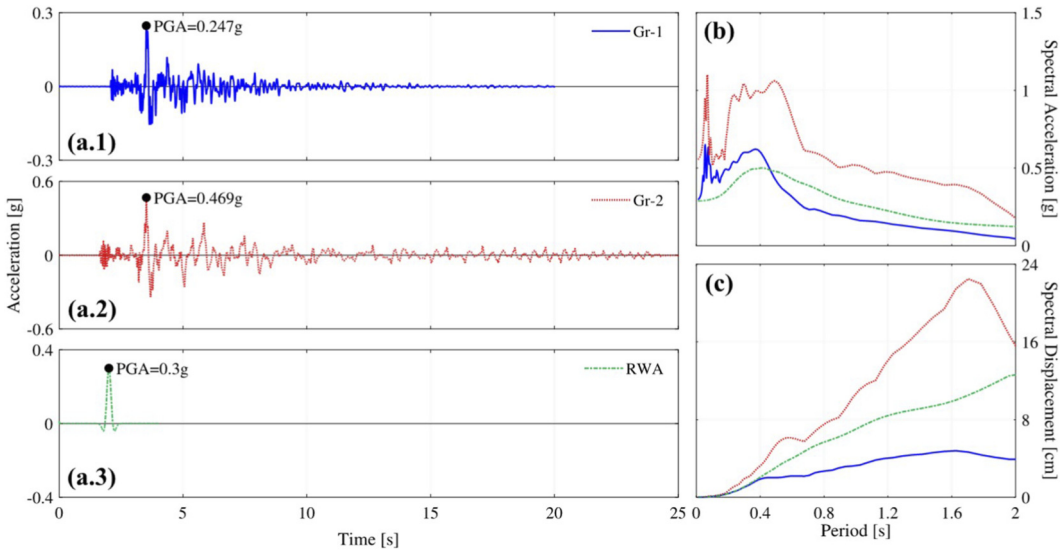


FIGURE 5
Overview of the loading input signals used in dynamic simulations, adapted from (Graziotti et al., 2016): acceleration time histories of the input motions and their 5%-damped acceleration **(b)** and displacement **(c)** spectra of **(a.1)** Gr-1, **(a.2)** Gr-2, and **(a.3)** RWA signals. The "PGA" abbreviation stands for peak ground acceleration.

step added after the initial 0.3 MPa pre-compression and before the first dynamic run. During the transition between dynamic run sequences, specifically for the reduction in vertical pre-compression to 0.1 MPa, the wall is maintained at its final position from the last run under moderate pre-compression (Run 13). At this stage, vertical uplift, lateral IP or OOP translations (the

latter when IP tilting is applied and the former when OOP tilting is considered), and OOP or IP rotation (the latter when IP tilting is applied and the former when OOP tilting is considered) DoFs at the top reference point are released. The vertical overburden is then reduced, the original dynamic boundary conditions are reinstated, and the subsequent loading history is applied.

Dynamic loading in each run is applied using the same boundary conditions as those used in the pushover analyses, with the acceleration time histories shown in Figure 5 applied to the translational DoF of the base and top reference points along the z-direction (Figure 4b.2). These signals, introduced in (Ghezelbash et al., 2025b) and used in the reference one-way bending OOP experiment (Graziotti et al., 2016), are briefly described here for completeness. The Gr-1 signal represents ground-level motion due to induced seismicity in the Groningen region of Netherlands at the time the experiments were conducted. The Gr-2 record corresponds to the first-floor response extracted from the numerical model of a two-story building subjected to the Gr-1 input at its base. The third signal is a synthetic 2 Hz Mexican hat pulse, also known as the Ricker Wavelet (RWA). All signals are applied in full, without cropping their low-amplitude start and end portions. It is important to note that for walls with OOP base tilting, the direction of dynamic loading remains fixed and horizontal along the z-axis. This reflects real-world conditions, where seismic input maintains a global direction, even as the walls themselves deform OOP due to initial base tilting.

2.6 Limitations of the parametric study

The current parametric study is intended as an exploratory investigation, and it incorporates several simplifications that are discussed below.

First, while the primary objective of this study, and the key utility of the modeling approach developed by the authors (Ghezelbash et al., 2025b) is to investigate the dynamic OOP behavior of URM walls, the majority of the variations are analyzed via static OOP pushover. This choice primarily serves to simplify the procedure and to enable a more comprehensive investigation of parameters such as vertical overburden as explained in the following. The dynamic loading sequence used in this study is based on the reference experiment from the EUCENTRE campaign (Graziotti et al., 2016), which was tailored to the specific vertical loading conditions of the tested specimen. Adapting the sequence to each variation in this parametric study would require additional modifications and iterative trial-and-error to ensure suitability. To bypass this challenge, the variations with different vertical overburdens introduced in Section 2.3 are analyzed through static pushover loading, while dynamic analysis is reserved for configurations that replicate the specific vertical loading setup used in the original experiment. Additionally, the dynamic sequence already includes two stages of vertical overburden, 0.3 MPa followed by 0.1 MPa, which align closely with the moderate (0.25 MPa) and low (0.1 MPa) pre-compression levels considered in the pushover analyses. This allows for sufficient coverage of potential dynamic responses under these representative conditions. As noted in Section 2.3, the high pre-compression level, which is not included in the dynamic sequence, is only intended as an extreme case to activate crushing in the expanded blocks and does not reflect real-world conditions typical of the low-rise buildings whose behavior is intended to be studied here (Gonen et al., 2023). Therefore, its exclusion from the dynamic regime is not expected to limit the overall practical relevance of the parametric study. Moreover, static pushover analyses are widely used in the literature as cost-effective alternatives to dynamic time-history simulations for investigating seismic behavior (Guettala et al., 2025b), and are considered to provide sufficiently reliable information on key response parameters, including stiffness, strength, deformation capacity, and failure mechanisms under real-world earthquakes.

Second, although base tilting induces relative drift at the wall top with respect to the base, the top is subsequently held fixed during pushover loading or is prescribed dynamic motions identical to the base. This setup deviates from real-world conditions, where second-order effects from the superstructure can lead to progressive top deformations both prior to and during OOP loading. However, the boundary conditions used in this study are intentionally simplified to facilitate interpretation and enable clearer comparisons. For example, they eliminate the interaction of the applied OOP loading with the amount of base tilt, i.e., the gradual increase in tilt during OOP loading, which would otherwise complicate the quantification of OOP responses. Moreover, considering that this study serves as a complement to experimental efforts, the numerical simulations can be interpreted as artificial experiments. In reality, no experimental studies of the tilted walls exist in the literature, eliminating the possibility of the calibration of the modeling approach against more realistic conditions. Not only that, if physical testing were conducted on walls under base tilting, similar idealizations of boundary conditions would be required to ensure feasibility (Dauda et al., 2024). Moreover, free relative motion of the top is more appropriate for parapets walls and self-standing towers rather than walls of a building supported by diaphragms at their upper levels (Sorrentino et al., 2016). Future studies should extend the investigation to larger facades, where the use of simplified boundary conditions is no longer necessary. Examining OOP dynamic behaviors under differential boundary motions is also crucial to replicate conditions of upper floors walls, which are expected to also be more sensitive to base tilting effects due to lower vertical confinement (see (Ghezelbash et al., 2025d)). Furthermore, the top fixity condition can be refined by incorporating elements that more accurately capture wall-diaphragm interactions, including possible detachment.

Third, although real earthquakes impose multi-directional excitation on structures, namely, in the lateral IP and OOP directions and in the vertical direction, the analyses in this study consider only the lateral OOP component. This assumption is adopted to simplify the problem and isolate the effects under investigation. Specifically, incorporating lateral IP and vertical seismic components would require more realistic IP boundary conditions at the wall tops to permit proper deformation, which have not been adopted for the reasons discussed in the previous paragraph. In addition, the presence of these components during the excitation of tilted walls would introduce further complex phenomena, hindering the accurate identification of the effects of tilting on seismic response. Future studies, particularly those addressing full façades and towers, should therefore investigate the influence of base tilting under IP seismic loading as well as

under multi-directional earthquake excitation (Mazza and Labernarda, 2023).

Fourth, a single maximum limit of OOP base tilting is applied uniformly to all wall specimens, based on the stability threshold of the most vulnerable configuration, rather than determining an individual limit for each case. This approach is adopted to simplify the study procedure and to ensure a consistent initial condition across all specimens, thereby facilitating direct comparison of the results. This decision is further supported by the specific geometries of the walls studied. As previously noted, the maximum OOP base tilt produces an OOP drift equivalent to 22% of the wall thickness, approaching the 25% collapse threshold identified in previous works of the authors (Ghezelbash et al., 2025a). While higher tilt values might have been feasible for some configurations under low or moderate pre-compression, they would exceed the practical range of rotations observed in real structures. In fact, even the large OOP drift considered here is made possible by the idealized boundary conditions used in the study, which maintain a fixed relative OOP displacement between the top and base of the wall. In a real construction, a wall not constrained at its top (such as a parapet) experiencing such drift would likely collapse under relatively low dynamic excitation, due to the substantial second-order effects induced by gravity and vertical overburden (Doherty et al., 2002; Griffith et al., 2003; Robazza et al., 2018). Moreover, walls with such large residual OOP displacements are typically classified, based on visual inspection alone, as high-risk in current post-earthquake assessment practice. In other words, they are commonly marked as unusable or conditionally usable only after repair or temporary countermeasures, and they must be rehabilitated before being deemed safe for future seismic events (FEMA 306: Evaluation of Earthquake Damaged Concrete and Masonry Wall Buildings, 2000; Taucer and Pinto Vieira, 2007; Burton and Deierlein, 2018; Di Ludovico et al., 2021).

Fifth, the parametric study considers only one-way spanning walls and the effects of base tilting on two-way bending OOP behavior are not investigated. This simplification is made primarily because base tilting is less relevant for two-way spanning walls, as discussed in the following. Both IP and OOP base tilting influence OOP response by altering vertical confinement, that is, modifying arching effects. One-way spanning walls are particularly sensitive to such changes, as their response is primarily governed by the effectiveness of vertical arching (see (Ghezelbash et al., 2025d) for further details). In contrast, two-way spanning walls benefit from additional horizontal arching and brick interlocking with intersecting walls perpendicular to them, which is expected to make them less vulnerable to base tilting. Moreover, base tilting is generally a byproduct of ground settlement. Under varying subsidence profiles, two-way spanning walls tend to undergo more severe internal deformations due to their greater length and the added influence of intersecting elements, which increase their susceptibility to the imposed ground curvature (Prosperi et al., 2023c; 2023b). Meanwhile, significant base tilting is typically observed in walls with relatively short lengths compared to the subsidence profile, or in one-way spanning walls that are not laterally confined by perpendicular elements (Charles and Skinner, 2004; Prosperi et al., 2023b; Kolivand and Daraei, 2024). Accordingly, this study focuses on one-way spanning specimens to examine the effects of base tilting, while reserving the investigation of two-way spanning walls for a more comprehensive study in the future works, where a more realistic settlement loading approach is adopted.

Sixth, the study considers only a limited range of wall geometries and one specific set of material properties, which may restrict the generalizability of the findings. In terms of geometry, although the wall lengths considered are representative of isolated walls in real buildings, longer walls would be more suitable for representing full façades with lower height-to-length ratios. More importantly, the absence of geometrical variations involving one or more window or door openings, or their combination, remains a limitation. Such openings may induce local phenomena, including cracking or crushing at the corners, particularly under IP tilting, and may therefore amplify subsequent effects on OOP response. Regarding materials, the specimens represent walls with strong units and strong mortar, with damage occurring mainly in the mortar (Graziotti et al., 2016; Ghezelbash et al., 2025b). Although this combination is representative of buildings in Groningen (Jafari et al., 2019), its applicability to other URM typologies remains uncertain. For example, walls with weak units and strong mortar, such as those tested in (Sajid et al., 2018), may be more vulnerable to base tilting. Hence, further investigations considering a wider range of wall geometries and material properties are required to draw more general conclusions.

In light of the limitations discussed above, the results of this study should be regarded as preliminary insights as the objective has not been to provide a generalizable answer to the effects of base tilting on seismic response, but rather to establish a foundational methodology for future investigations and to identify key limitations that should be addressed in subsequent studies.

3 Simulation results

The results of the 31 analyses conducted in the parametric study are presented in this section, covering OOP load-deformation responses from pushover analyses, peak OOP displacements recorded during each dynamic loading run, and the collapse mechanisms of all specimens. Quantitative results and damage patterns from simulations under IP base tilting are shown in Figures 6, 7, respectively, while those from simulations under OOP base tilting are presented in Figures 8, 9. In Figures 6, 8, simulations without base tilting are represented by black lines, and those with base tilting are shown in color. For the pushover results, all curves are normalized to the peak OOP strength of the non-tilted variation to facilitate direct comparison. In dynamic analyses, collapse events are indicated with cross (×) marks. In Figure 8, dynamic results without base tilting are presented for both wall geometries: the "Short wall" is shown with a solid black line and the "Long wall" with a dotted black line, highlighting their differing responses due to geometric variation. The deformed shapes in Figures 7, 9 are scaled with different factors for clarity. For pushover analyses in the negative z-direction, the deformed shapes are rotated by 90° about the vertical axis to visualize the back of the walls. Finally, compressive damage in the expanded blocks is highlighted in red.

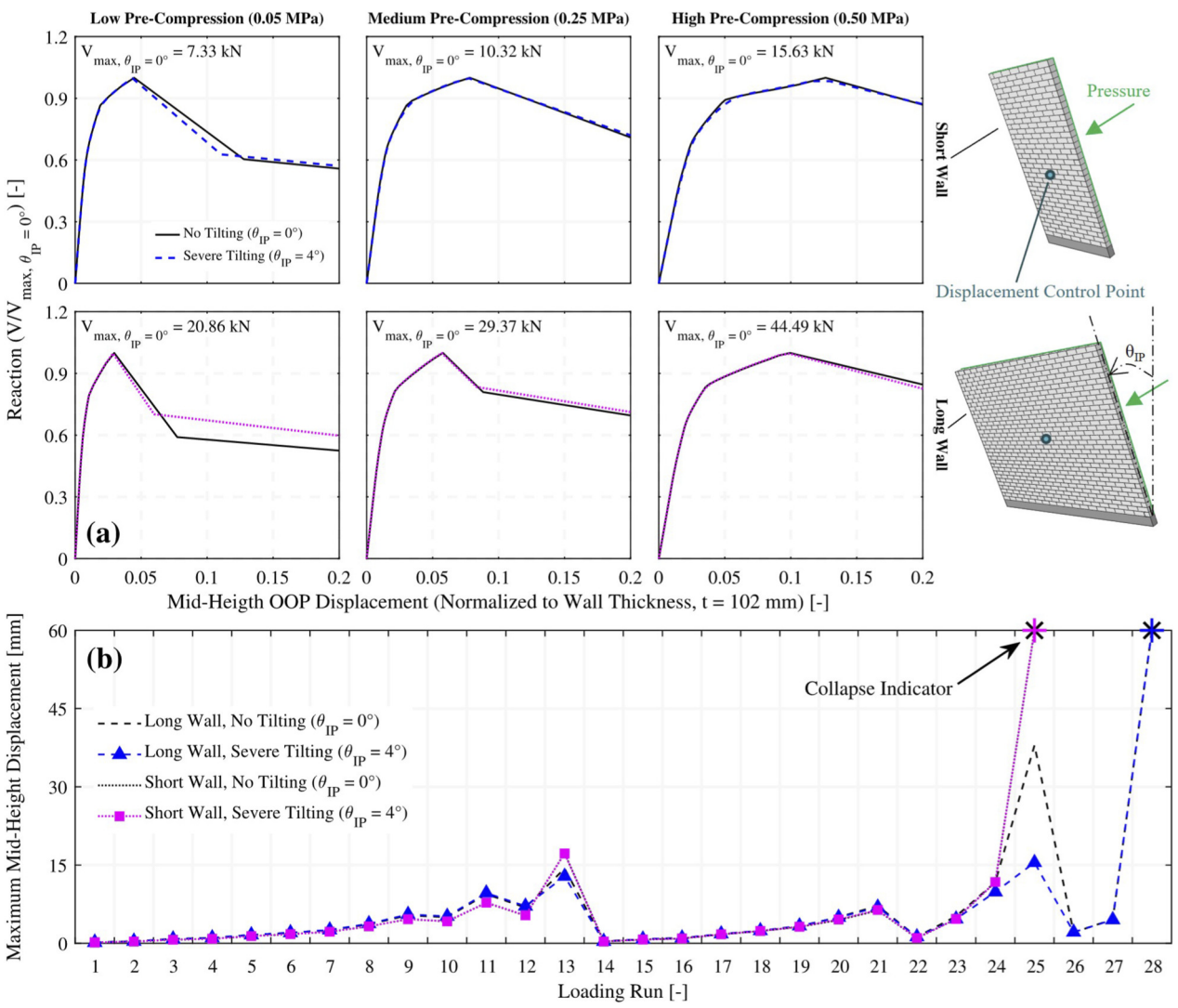


FIGURE 6
The results of pushover **(a)** and dynamic **(b)** analyses under different levels of IP base tilting. The collapse in dynamic simulations is highlighted with a cross (×) mark.

4 Discussion of the observations

The specimens exhibit very low sensitivity to IP base tilting in both pushover and dynamic analyses, as shown in Figure 6. In pushover, load-deformation responses remain largely unchanged, with only minor variations in post-peak behavior observed in specimens under low pre-compression. In dynamic simulations of the Short wall, although the tilted variation exhibits slightly different deformation demands, both tilted and non-tilted walls collapse at the same loading run. Similarly, both non-tilted and tilted Long walls collapse during the same dynamic loading run, although it being three runs earlier than the Short wall, possibly due to the influence of new deformation modes introduced by the greater length of these walls. Moreover, the tilted Long wall shows the same amount of run-by-run maximum deformations as its non-tilted counterpart. This negligible difference in the response of non-tilted and IP-tilted walls is also reflected in the collapse mechanisms illustrated in Figure 7, where all tilted walls exhibit nearly identical failure patterns to their non-tilted counterparts. Minor differences are observed in the pushover failure mechanisms. For example, in the Short wall under the lowest pre-compression, the non-tilted variation shows a typical single-joint-row failure, while the rotated version exhibits a stepped crack path involving two joint rows at its mid-height. Slightly more pronounced differences appear in the Long wall. Under low pre-compression, the tilted wall displays an additional diagonal crack passing through the joints on its less compressed (right) side, along with sliding of the mid-height joint on the more compressed (left) side. Under moderate pre-compression, the tilted variation develops a step in its mid-height horizontal crack and delamination of several blocks near the less compressed (right) edge. Under high pre-compression, both tilted and non-tilted Long walls exhibit similar damage patterns.

Slightly greater sensitivity to OOP base tilting is observed. As shown in Figure 8a, the pushover curves of walls with moderate tilting (0.4% drift) show close agreement with the non-tilted responses, while minor deviations are observed in those with

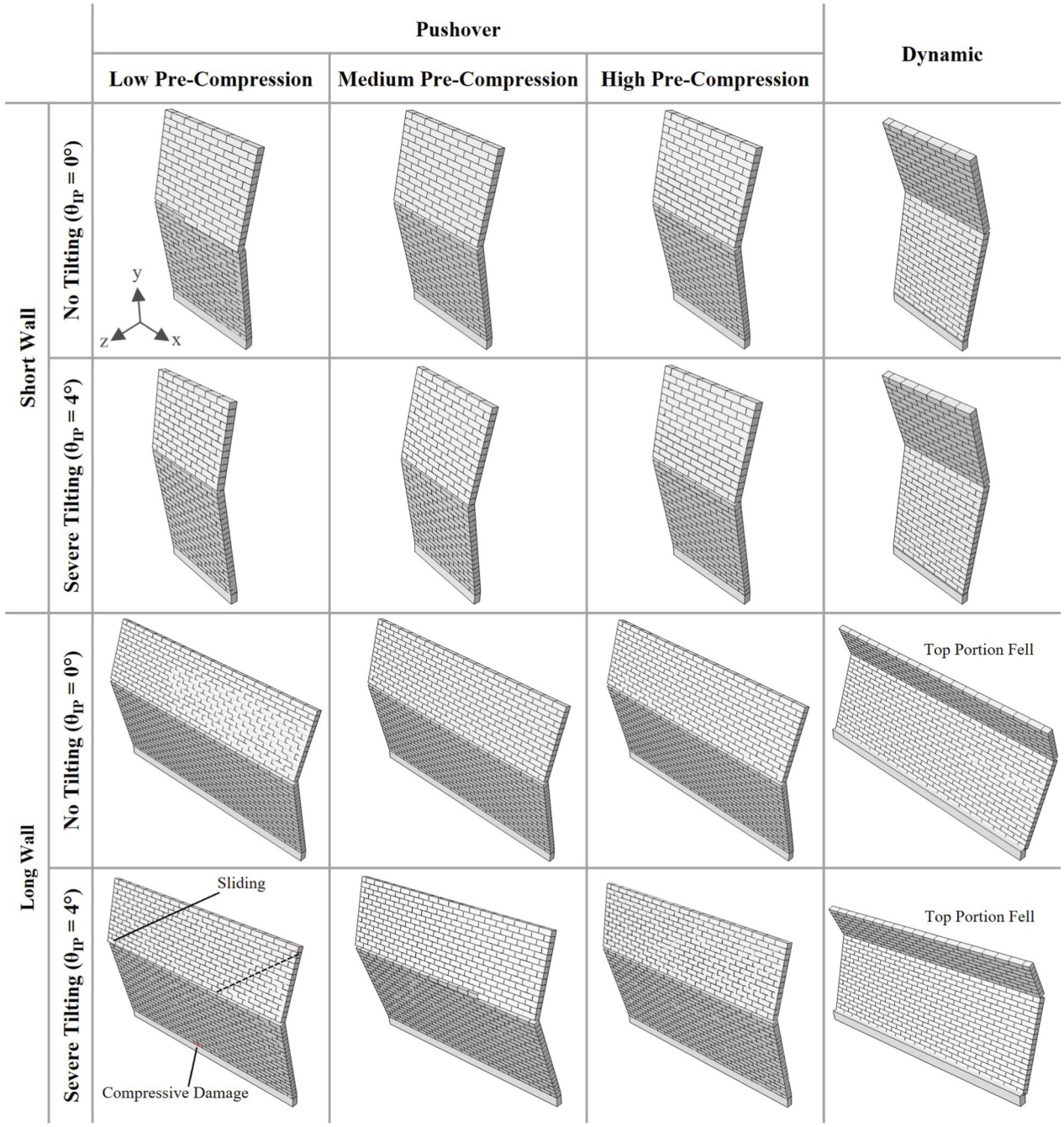


FIGURE 7
Collapse mechanisms of simulations with IP base tilting. The deformed shapes are scaled with different factors for clear visualization. Compressive damage in the blocks is highlighted in red.

severe tilting (0.8% drift). For the latter, while these deviations are almost non-existent under low pre-compression, the walls with moderate pre-compression show slightly different peak strengths and the ones under high-pre-compression also exhibit slightly lower stiffnesses. As previously discussed, the larger sensitivity of walls with high pre-compression to OOP tilting is expected, given the strong influence of vertical confinement on the OOP response of one-way spanning walls. When vertical confinement is low, base rotation has a limited effect; however, at higher pre-compression levels, the change in the alignment of the vertical force with the wall plane due to base tilting results in a greater reduction of the effective vertical confinement, thereby weakening the response more significantly. This is particularly evident in the wall under high pre-compression subjected to reverse pushover loading (towards its original plane). As discussed in Section 2.4, this configuration is the most vulnerable to OOP base tilting and shows the lowest tilting capacity. The severe base rotation, being close to the instability threshold of the wall, leads to a more noticeable reduction in stiffness, possibly due to the facilitation of cracking under subsequent OOP loading. A directional sensitivity is also noted,

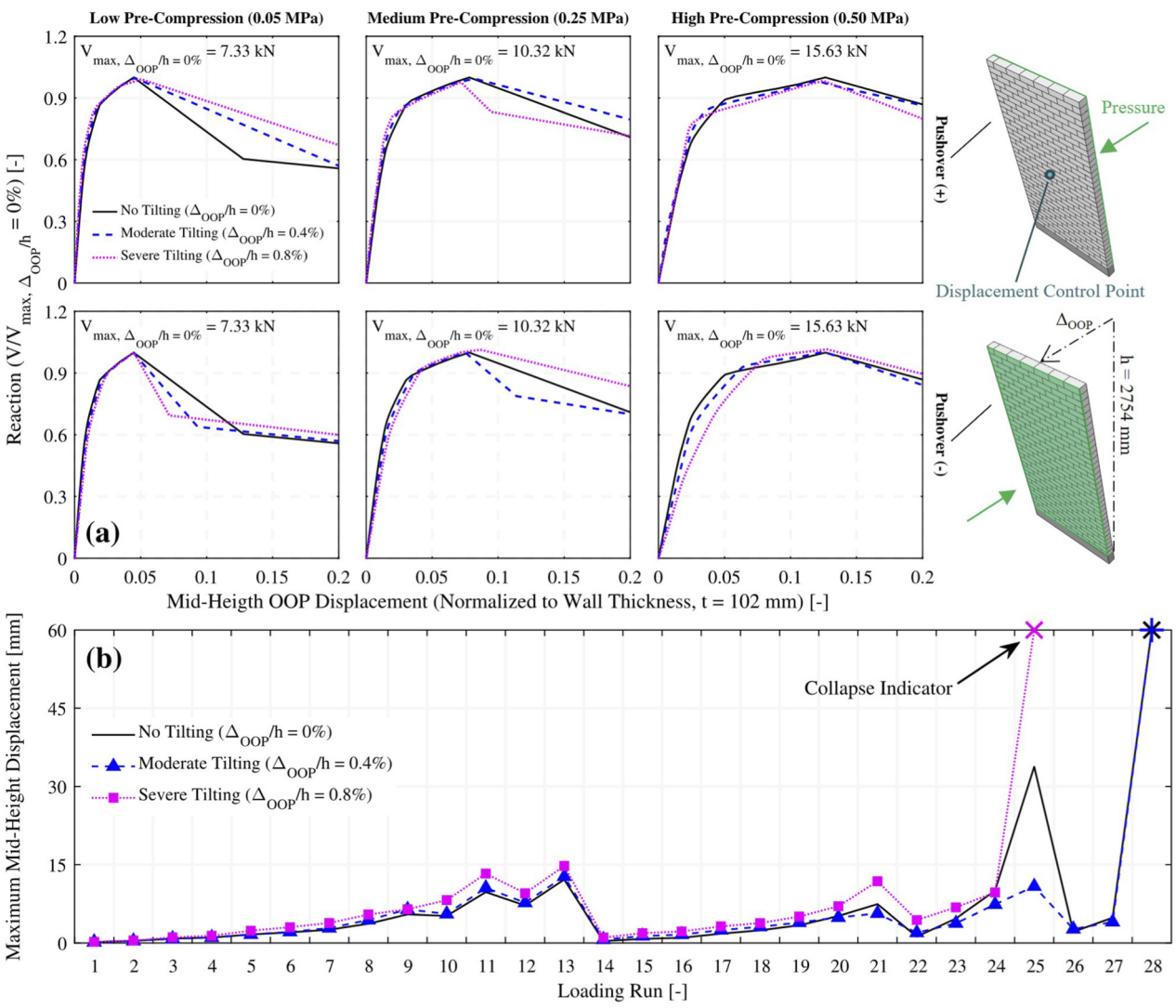


FIGURE 8
The results of pushover **(a)** and dynamic **(b)** analyses under different levels of OOP base tilting. The collapse in dynamic simulations is highlighted with a cross (×) mark.

with walls generally exhibiting lower stiffness when pushed toward their original position (negative z-direction).

In the dynamic simulations (Figure 8b), the wall with moderate base tilting exhibits deformation demands nearly identical to its non-tilted counterpart and collapses at the same loading run. This observation aligns with the findings reported in (Al Shawa et al., 2012), where OOP base tilting resulting in top displacements up to 8% of wall thickness has had no significant effect on the dynamic rocking response of single blocks. However, the wall with severe base tilting shows higher peak displacements even during the low-amplitude loading runs and collapses three runs earlier than the other two specimens. This highlights not only the increased sensitivity of dynamic response to base tilting, even under low and moderate pre-compression, but also the distinct behavior that arises when the orientation of the wall relative to the applied loads is altered. A simplified visual explanation is provided in Figure 10. During OOP base tilting, all actions applied to the wall (gravity, vertical overburden, and dynamic ground motion) are decomposed into two components relative to the tilted plane of the wall. One component is perpendicular to the plane of the wall, and one is parallel to it. The perpendicular components (Figure 10a) of gravity and vertical load act in the direction of OOP rotation, while the parallel components (Figure 10b) act along the wall height and contribute to vertical confinement. This decomposition influences the OOP response in three ways. First, the perpendicular component of gravity adds to the perpendicular component of ground motion, potentially increasing the overall OOP load and leading to earlier collapse. Second, the reduction in vertical confinement, due to misalignment of the overburden, lowers wall stiffness, thereby increasing deformation, as also seen in the pushover responses (Figure 8a). Third, during phases of the dynamic motion when the parallel acceleration is directed upward, it can act opposite to gravity and overburden, further reducing the effective vertical confinement. This interaction may temporarily compromise the resistance of the wall, especially during the peaks of the ground motion, increasing the likelihood of strength loss and early collapse.

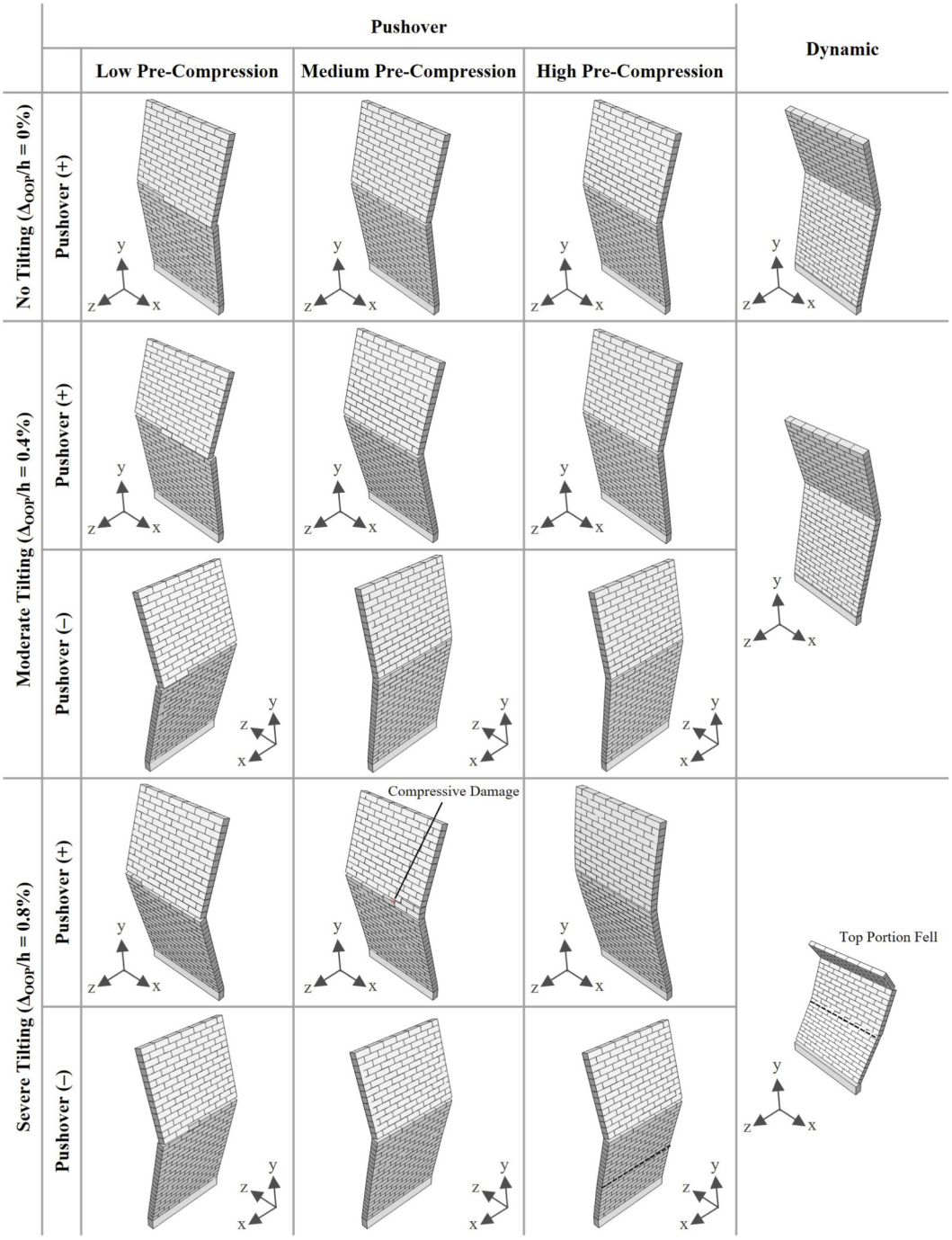


FIGURE 9
Collapse mechanisms of simulations with OOP base tilting. The deformed shapes are scaled with different factors for clear visualization. Compressive damage in the blocks is highlighted in red.

These effects occur regardless of the applied pre-compression level, diminishing the relative importance of vertical confinement in the dynamic regime. However, the wall with lower pre-compression regime appears more affected in this study, as dynamic loading is more likely to induce uplift and fluctuations in vertical confinement in this regime than in the case with moderate pre-compression. It should further be noted that such an effect on uplift is not observed in pushover analyses as the static loading pressure is always kept perpendicular to the surface of the wall, and such decomposition of OOP load does not occur therein.

The effects of OOP base tilting are also evident in the failure mechanisms presented in Figure 9. In the pushover analyses, collapse mechanisms of walls under low pre-compression are nearly identical across rotated and non-rotated cases. In contrast, walls with moderate pre-compression show slightly more variations, and those with high pre-compression exhibit the most pronounced

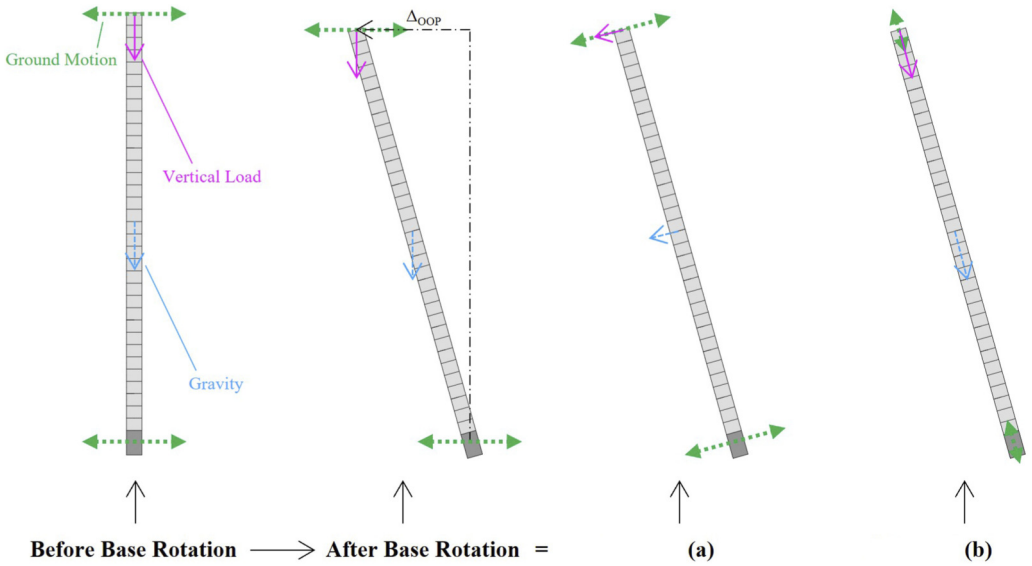


FIGURE 10
Schematic visual illustration of the effect of OOP base tilting on the loads experienced by the walls during dynamic loading. A side view of the Short wall is presented. **(a)** Perpendicular +.. **(b)** Parallel actions.

differences. These trends reflect the corresponding changes observed in the load-deformation responses (Figure 8a). For example, the severely tilted wall under moderate pre-compression develops an additional stepped crack and localized compressive damage when pushed in the positive z-direction, which accounts for its slightly reduced strength compared to its less- and non-rotated counterparts. Similarly, the severely tilted wall under high pre-compression exhibits an additional crack at approximately one-quarter of its height when loaded in the negative z-direction. This corresponds to the lower stiffness observed in its load-deformation response and may indicate minor damage initiated during the base tilting phase. The same crack is also observed in the dynamic analysis of the severely rotated wall, further underscoring the influence of load orientation on collapse mechanisms and structural strength.

Although the observations reported in this section are considered valid, they cannot be generalized due to the limited number of simulations, the use of a single loading sequence for the dynamic analyses, and the specific material properties used, and the idealized boundary conditions adopted in the study, as discussed in Section 2.6. Nevertheless, two clear outcomes are noted. First, simulations under IP base tilting reveal slightly higher sensitivity in walls with low pre-compression and those with larger lengths. In the former, low vertical confinement results in reduced shear resistance at the joints, particularly due to limited frictional contribution, thereby facilitating shear sliding in joints already cracked in flexure. In the latter, IP base tilting leads to greater redistribution of vertical stresses than in shorter walls, producing reduced confinement on one side and increased confinement on the other. In walls with high pre-compression, such effects are mitigated, as the overall magnitude of confinement is sufficient to override stress redistribution. However, the sensitivity is minimal for all the performed simulations. Second, both high and low pre-compression walls show sensitivity to OOP base tilting. In high pre-compression cases, base tilting introduces significant changes in vertical confinement, resulting in notable stiffness reduction under pushover loading. In low pre-compression walls, the OOP component of (dynamic) loading more readily induces uplift and loss of vertical confinement compared to cases with moderate pre-compression. This suggests the existence of a threshold level of pre-compression, with OOP base tilting degrading the one-way bending OOP response both above and below this threshold.

It is important to note that such effects of wall orientation relative to ground motion, i.e., changes in the uplift as a result of a parallel component of dynamic action, are not observed in studies on the OOP behavior of two-way spanning walls (Sharma et al., 2020). This is because their two-way bending response is governed by flexural and shear failure mechanisms that are less sensitive to vertical confinement and benefit from additional horizontal confinement (Graziotti et al., 2017; Chang et al., 2020). Therefore, the findings presented here are limited to one-way spanning walls, which are more affected by variations in vertical confinement. This distinction further supports the focus of the current study on one-way spanning walls. Moreover, previous studies (Di Michele et al., 2020; Al Shawa et al., 2023) confirm that dynamic OOP behavior, even at the building scale, is sensitive to the vertical component of ground motion. Consequently, the low sensitivity of the two-way spanning walls in (Sharma et al., 2020) may be attributed to the specific spectral characteristics of the loading signals used, which may not have caused significant amplification in the dynamic response (Kallioras et al., 2022).

5 Conclusion

This paper presents a preliminary investigation into the out-of-plane (OOP) response of unreinforced masonry (URM) walls subjected to base tilting induced by ground settlement. The high-

fidelity modeling approach developed by the authors is applied to simulate such scenarios, which are largely unexplored in the existing literature. A parametric study is conducted on two wall geometries: one short wall with a high height-to-length aspect ratio (h/l = 1.9), and one long wall with a moderately low aspect ratio (h/l = 0.67), both representative of typical real-world construction. The walls are subjected to two types of base tilting, in-plane (IP) and OOP, followed by an OOP loading phase. OOP behavior is analyzed both in the static regime, through unidirectional pushover analyses, and in the dynamic regime, by applying real earthquake ground motions to the wall boundaries. Pushover simulations are repeated under varying levels of vertical overburden, representing conditions found in top- and ground-floor walls of low-rise two-story buildings, as well as in highly compressed configurations with potential for crushing failure. Dynamic analyses follow a multi-step loading sequence from a benchmark experiment, against which the modeling approach has been originally calibrated. IP base tilting is applied using a single large 4° rotation value across all variations, representative of the most severely tilted real-world structures. OOP base tilting is studied at two levels, moderate with 0.4% OOP drift at the top of the walls and severe with 0.8% drift, the latter being close to the stability threshold of the specimens. The results are interpreted in terms of the influence of base tilting on static load-deformation response, dynamic deformation demands and collapse onset, and failure mechanisms. The main findings are as follows:

- The specimens studied here showed minimal sensitivity to IP base tilting, despite the large value (4°) of the applied rotation. This may have been resulted from the simplified boundary conditions used, where the wall top was prevented from developing additional displacement relative to the base after initial tilting, i.e., progressive tilting during OOP loading was not considered.
- Under IP base tilting, only walls with low pre-compression exhibited minor variations in collapse mechanisms. These differences were primarily aesthetic and did not alter the dominant failure mode in the walls studied here. Longer walls showed more of these minor changes than shorter ones, likely due to more effective redistribution of vertical stresses resulting from their greater length.
- Specimens subjected to OOP base tilting displayed greater sensitivity. However, the moderate tilting level considered here did not affect the response and only severe tilting, equal to an OOP drift at the wall top equal to 22% of wall thickness, caused slightly reduced pushover stiffness, increased dynamic deformation demands, and early dynamic collapse. In-between tilting levels, not considered here, may demonstrate different behaviors.
- In static pushover, severe base tilting was particularly detrimental for walls with high pre-compression, as it approached the stability threshold for OOP overturning. This condition facilitated cracking during subsequent OOP loading and induces more substantial changes in vertical confinement compared to less-compressed walls.
- In dynamic regime, walls with low pre-compression were also affected by OOP base tilting, primarily due to the change in wall orientation relative to applied loads. The rotated condition introduced a gravity component acting in the direction of tilt and a dynamic loading component that opposed vertical overburden, thereby increasing the OOP action and reducing confinement, respectively.

This study extends the current knowledge in the literature by demonstrating that one-way spanning walls may be particularly sensitive to OOP base tilting. It provides artificial experiments that complement existing physical tests conducted on non-tilted one-way spanning walls. However, since the study presents a preliminary analysis based on specimens representing a limited subset of real-world structures in terms of material and geometry, and adopts simplified loading and boundary conditions, the findings may not be fully generalizable, and the identified limitations should be addressed in future work. Particularly, further investigations are needed to include additional wall specimens with varying material properties and geometries. Moreover, future studies should expand the scope of dynamic simulations, both by incorporating additional loading signals beyond those used here, and by adopting an incremental dynamic approach instead of a sequential loading procedure. Additionally, the simulation of larger facades with more realistic post-tilting boundary conditions is necessary. Specifically, future works should considered differential boundary motions as well as the progression of tilting during OOP loading by the inclusion of wall diaphragm interactions. Another important extension could be the inclusion of the vertical component of earthquakes in dynamic analyses, considering its potential contribution to the further reduction of confinement in walls exhibiting OOP tilting. These extensions would support the development of probabilistic frameworks capable of capturing the uncertainties inherent in dynamic responses, which are often governed by complex, chaotic behavior.

Data availability statement

The original contributions presented in the study are included in the article/supplementary material, further inquiries can be directed to the corresponding author.

Author contributions

AG: Writing – review and editing, Investigation, Writing – original draft, Conceptualization, Data curation, Visualization, Formal Analysis, Software, Resources, Validation, Methodology. JR: Writing – review and editing, Supervision, Validation, Resources, Conceptualization, Funding acquisition. FM: Resources, Validation, Conceptualization, Project administration, Writing – review and editing, Funding acquisition, Supervision.

Funding

The author(s) declared that financial support was received for this work and/or its publication. This research was conducted as part of the scientific consolidation of projects funded by Nederlandse

Aardolie Maatschappij (NAM) BV under contract number UI46268 "Physical testing and modeling-Masonry structures Groningen", which is gratefully acknowledged. The funder was not involved in the study design, collection, analysis, interpretation of data, the writing of this article, or the decision to submit it for publication.

Acknowledgements

The loading signals used for the dynamic simulations of this study are adapted from the experimental campaign conducted at EUCENTRE foundation (Pavia, Italy) on one-way spanning full-scale URM walls (Graziotti et al., 2016).

Conflict of interest

The author(s) declared that this work was conducted in the absence of any commercial or financial relationships that could be construed as a potential conflict of interest.

Generative AI statement

The author(s) declared that generative AI was not used in the creation of this manuscript.

Any alternative text (alt text) provided alongside figures in this article has been generated by Frontiers with the support of artificial intelligence and reasonable efforts have been made to ensure accuracy, including review by the authors wherever possible. If you identify any issues, please contact us.

Publisher's note

All claims expressed in this article are solely those of the authors and do not necessarily represent those of their affiliated organizations, or those of the publisher, the editors and the reviewers. Any product that may be evaluated in this article, or claim that may be made by its manufacturer, is not guaranteed or endorsed by the publisher.

References

Al Shawa, O., de Felice, G., Mauro, A., and Sorrentino, L. (2012). Out-of-plane seismic behaviour of rocking masonry walls. *Earthq. Eng. Struct. Dyn.* 41, 949–968. doi:10.1002/eqe.1168

Al Shawa, O., Liberatore, D., and Sorrentino, L. (2023). Effect of the vertical component of ground motion on a rubble masonry wall model. *Procedia Struct. Integr.* 44, 1396–1402. doi:10.1016/j.prostr.2023.01.179

ASCE 41-17: Seismic Evaluation and Retrofit of Existing Buildings (2017). *Seismic evaluation and retrofit of existing buildings*. Reston, VA, USA: American Society of Civil Engineers ASCE.

Burland, J. B., Jamiolkowski, M. B., and Viggiani, C. (2009). Leaning tower of Pisa: behaviour after stabilization operations. *Int. J. Geoengin. Case Histories* 1, 156–169.

Burton, H. V., and Deierlein, G. G. (2018). Integrating visual damage simulation, virtual inspection, and collapse capacity to evaluate post-earthquake structural safety of buildings. *Earthq. Eng. Struct. Dyn.* 47, 294–310. doi:10.1002/eqe.2951

Canadian Standards Association (2004). *S304.1-04: Design of masonry structures*. Mississauga, ON, Canada.

Canditone, C., Parisi, F., D'Ayala, D. F., and Guardiola-V, A. (2025). Seismic collapse analysis of unreinforced masonry buildings through applied element micro-modelling and crack width-based damage measures. *Bull. Earthq. Eng.* 23, 4719–4753. doi:10.1007/s10518-025-02231-9

Chang, L., Messali, F., and Esposito, R. (2020). Capacity of unreinforced masonry walls in out-of-plane two-way bending: a review of analytical formulations. *Structures* 28, 2431–2447. doi:10.1016/j.istruc.2020.10.060

Charles, J. A., and Skinner, H. D. (2004). Settlement and tilt of low-rise buildings. *Proc. Institution Civ. Eng. - Geotechnical Eng.* 157, 65–75. doi:10.1680/geng.2004.157.2.65

Choi, Y., Park, D., Kim, S., and Hong, J. W. (2023a). Investigation on the behavior factor of leaning masonry wall structures. *Bull. Earthq. Eng.* 21, 2987–3009. doi:10.1007/s10518-023-01646-6

Choi, Y., Park, D., Kim, S., Jin, S., and Hong, J. W. (2023b). Experimental and numerical analyses of seismic behaviors of L-shaped unreinforced masonry walls. *Eng. Struct.* 297, 116989. doi:10.1016/j.engstruct.2023.116989

Cito, P., Chioccarelli, E., and Iervolino, I. (2022). Macroseismic intensity hazard maps for Italy based on a recent grid source model. *Bull. Earthq. Eng.* 20, 2245–2258. doi:10.1007/s10518-022-01323-0

Crowley, H., Pinho, R., Polidoro, B., and van Elk, J. (2017). Developing fragility and consequence models for buildings in the Groningen field. *Neth. J. Geosciences* 96, s247–s257. doi:10.1017/njg.2017.36

Damiani, N., Bertassi, M., Sharma, S., Smerilli, M., Mirra, M., Lanese, I., et al. (2025). Out-of-Plane shake-table tests on unreinforced masonry gables considering different roof configurations. 268–279. doi:10.1007/978-3-031-98893-6_25

Danciu, L., Nandan, S., Reyes, C., Basili, R., Weatherill, G., Beauval, C., et al. (2021). The 2020 update of the european seismic hazard model: Model overview.

Danciu, L., Giardini, D., Weatherill, G., Basili, R., Nandan, S., Rovida, A., et al. (2024). The 2020 european seismic hazard model: overview and results. *Nat. Hazards Earth Syst. Sci.* 24, 3049–3073. doi:10.5194/nhess-24-3049-2024

Dauda, J. A., Iuorio, O., Muhit, I. B., and da Silva, L. C. M. (2024). Systematic review of experimental testing of masonry walls' failure: comparative analysis and future directions. *Eng. Fail. Anal.* 163, 108571. doi:10.1016/j.engfailanal.2024.108571

Derakhshan, H., Griffith, M. C., and Ingham, J. M. (2016). Out-of-plane seismic response of vertically spanning URM walls connected to flexible diaphragms. *Earthq. Eng. Struct. Dyn.* 45, 563–580. doi:10.1002/eqe.2671

Di Ludovico, M., De Martino, G., Prota, A., Manfredi, G., and Dolce, M. (2021). Damage assessment in Italy, and experiences after recent earthquakes on reparability and repair costs. 65–84. doi:10.1007/978-3-030-68813-4_4

Di Michele, F., Cantagallo, C., and Spacone, E. (2020). Effects of the vertical seismic component on seismic performance of an unreinforced masonry structures. *Bull. Earthq. Eng.* 18, 1635–1656. doi:10.1007/s10518-019-00765-3

Doherty, K., Griffith, M. C., Lam, N., and Wilson, J. (2002). Displacement-based seismic analysis for out-of-plane bending of unreinforced masonry walls. *Earthq. Eng. Struct. Dyn.* 31, 833–850. doi:10.1002/eqe.126

European Committee for Standardization (2004). *EN 1998-1: eurocode 8: design of structures for earthquake resistance - part 1: general rules, seismic actions and rules for buildings*. Brussels, Belgium.

FEMA 306: Evaluation of Earthquake Damaged Concrete and Masonry Wall Buildings (2000). *Evaluation of earthquake damaged concrete and masonry wall buildings*. Redwood City, CA, USA: Applied Technology Council. doi:10.1193/1.1586111

Ferreira, T. M., Costa, A. A., Vicente, R., and Varum, H. (2015). A simplified four-branch model for the analytical study of the out-of-plane performance of regular stone URM walls. *Eng. Struct.* 83, 140–153. doi:10.1016/j.engstruct.2014.10.048

Galanakis, N. (2019). *Determination of the displacement demand for the out-of-plane seismic response of unreinforced masonry walls for the Groningen case*. Delft, Netherlands: Delft University of Technology.

Ghezelbash, A., Messali, F., and Rots, J. G. (2023a). "Challenges in the calibration of finite element models for the analysis of masonry structures: a comparative study," in XVII International Conference on Computational Plasticity, Fundamentals and Applications (Barcelona, Spain).

Ghezelbash, A., Messali, F., and Rots, J. G. (2023b). "Finite element micro-modelling of masonry structures: calibration and analysis challenges," in Engineering Mechanics Institute (EMI) International Conference (Palermo, Italy).

Ghezelbash, A., Aşıkoğlu, A., D'Altri, A. M., Sharma, S., and Messali, F. (2025a). Blind prediction of the dynamic behavior of 3D-printed masonry-like structures under shake-table loading *via* a high-fidelity numerical modeling approach (under review). *Results Eng.*

Ghezelbash, A., D'Altri, A. M., Sharma, S., Lourenço, P. B., Rots, J. G., and Messali, F. (2025b). A block-based numerical strategy for modeling the dynamic out-of-plane

behavior of unreinforced brick masonry walls. *Meccanica* 60, 2069–2105. doi:10.1007/s11012-024-01899-8

Ghezelbash, A., Sharma, S., D'Altri, A. M., Lourenço, P. B., Rots, J. G., and Messali, F. (2025c). Challenges in high-fidelity implicit block-Based Numerical Simulation of dynamic out-of-plane two-way bending in unreinforced brick masonry walls. *Earthq. Eng. Struct. Dyn.* 54, 1836–1858. doi:10.1002/eqe.4337

Ghezelbash, A., Sharma, S., Rots, J. G., and Messali, F. (2025d). Effect of relative support motions on the out-of-plane dynamics of one-way spanning unreinforced masonry walls and insights into their instability displacement (under review). *J. Struct. Eng.*

Ghezelbash, A., D'Altri, A. M., Lourenço, P. B., and Miranda, S. de (2026). Numerical modeling of the out-of-plane dynamic response of masonry gable walls via a high-fidelity block-based finite element modeling approach – part I: blind prediction. *Bull. Earthq. Eng.* doi:10.1007/s10518-025-02328-1

Gonen, S., Pulatsu, B., Lourenço, P. B., Lemos, J. V., Tuncay, K., and Erduran, E. (2023). Analysis and prediction of masonry wallette strength under combined compression-bending *via* stochastic computational modeling. *Eng. Struct.* 278, 115492. doi:10.1016/j.engstruct.2022.115492

Graziotti, F., Tomassetti, U., Penna, A., and Magenes, G. (2016). Out-of-plane shaking table tests on URM single leaf and cavity walls. *Eng. Struct.* 125, 455–470. doi:10.1016/j.engstruct.2016.07.011

Graziotti, F., Tomassetti, U., Kallioras, S., Penna, A., and Magenes, G. (2017). Shaking table test on a full scale URM cavity wall building. *Bull. Earthq. Eng.* 15, 5329–5364. doi:10.1007/s10518-017-0185-8

Griffith, M. C., Magenes, G., Melis, G., and Picchi, L. (2003). Evaluation of out-of-plane stability of unreinforced masonry walls subjected to seismic excitation. *J. Earthq. Eng.* 7, 141–169. doi:10.1080/13632460309350476

Guettala, S., Abdesselam, I., Khelaifia, A., Guettala, S., and Chebili, R. (2025a). Advances in macro modeling for seismic performance assessment of infilled reinforced concrete structures. *Asian J. Civ. Eng.* 26, 1009–1022. doi:10.1007/s42107-024-01236-0

Guettala, S., Abdesselam, I., Rahmani, A. Y., Khelaifia, A., and Guettala, S. (2025b). Advancements in pushover analysis for improved seismic performance evaluation. *Archives Comput. Methods Eng.* 32, 4525–4554. doi:10.1007/s11831-025-10278-9

Jafari, S., Esposito, R., and Rots, J. G. (2019). From brick to element: investigating the mechanical properties of calcium silicate masonry. 596–604. doi:10.1007/978-3-319-99441-3_64

Kallioras, S., Graziotti, F., Penna, A., and Magenes, G. (2022). Effects of vertical ground motions on the dynamic response of URM structures: comparative shake-table tests. *Earthq. Eng. Struct. Dyn.* 51, 347–368. doi:10.1002/eqe.3569

Kesavan, P., and Menon, A. (2023). A macro-element with bidirectional interaction for seismic analysis of unreinforced masonry walls. *Earthq. Eng. Struct. Dyn.* 52, 1740–1761. doi:10.1002/eqe.3841

Koc, A. B., Erberik, M. A., Askan, A., and Karimzadeh, S. (2023). The sensitivity of global structural parameters for unreinforced masonry buildings subjected to simulated ground motions. *Buildings* 13, 2060. doi:10.3390/buildings13082060

Kolivand, F., and Daraei, A. (2024). The effect of masonry buildings' geometrical characteristics on their vulnerability caused by tunneling-induced settlement. doi:10.21203/rs.3.rs-4264070/v1

Korswagen, P. A., Longo, M., Prosperi, A., Rots, J. G., and Terwel, K. C. (2024). "Modelling of damage in historical masonry façades subjected to a combination of ground settlement and vibrations," in *Structural analysis of historical constructions* (Cham, Germany), 904–917. doi:10.1007/978-3-031-39603-8_73

Labernarda, R., and Mazza, F. (2026). Effects of the long-term degradation of fiber reinforced cementitious matrix (FRCM) systems on the seismic retrofitting of historical masonry structures. *Soil Dyn. Earthq. Eng.* 204, 110129. doi:10.1016/j.soildyn.2026.110129

Lourenço, P. B. (2000). Anisotropic softening model for masonry plates and shells. *J. Struct. Eng. (N. Y. N. Y).* 126, 1008–1016. doi:10.1061/(asce)0733-9445(2000)126:9(1008)

Malomo, D., and DeJong, M. J. (2022). A macro-distinct element model (M-DEM) for simulating in-plane/out-of-plane interaction and combined failure mechanisms of unreinforced masonry structures. *Earthq. Eng. Struct. Dyn.* 51, 793–811. doi:10.1002/eqe.3591

Mazza, F., and Labernarda, R. (2023). "Seismic retrofitting of framed structures by damped braces considering the out-of-plane response of masonry infills," in 9th International Conference on Computational Methods in Structural Dynamics and Earthquake Engineering (Athens, Greece), 2261–2270. doi:10.7712/120123.10558.20679

Messali, F., Esposito, R., Ravenshorst, G. J. P., and Rots, J. G. (2020). *Experimental investigation of the in-plane cyclic behaviour of calcium silicate brick masonry walls*. Netherlands: Springer. doi:10.1007/s10518-020-00835-x

Ministero delle Infrastrutture e dei Trasporti (2008). *NTC:2008, Decreto del Ministero delle infrastrutture*.

Ministero delle Infrastrutture e dei Trasporti (2018). *NTC:2018, Norme Tecniche per le Costruzioni*. Rome, Italy.

Namazi, E., and Mohamad, H. (2013). Potential damage assessment in buildings undergoing tilt. *Proc. Institution Civ. Eng. - Geotechnical Eng.* 166, 365–375. doi:10.1680/geng.10.00132

Netherlands Standardization Institute (2020). *NPR 9998:2020, assessment of structural safety of buildings in case of erection, reconstruction and disapproval - induced earthquakes - basis of design, actions and resistance*. Delft, Netherlands.

Nicodemo, G., Peduto, D., and Ferlisi, S. (2020). Building damage assessment and settlement monitoring in subsidence-affected urban areas: case study in the Netherlands. *Proc. Int. Assoc. Hydrological Sci.* 382, 651–656. doi:10.5194/piahs-382-651-2020

Noor-E-Khuda, S. (2021). An explicit finite-element modeling method for masonry walls using continuum shell element. *J. Archit. Eng.* 27, 04021040. doi:10.1061/(ASCE)AE.1943-5568.0000518

Noor-E-Khuda, S., Dhanasekar, M., and Thambiratnam, D. P. (2016). An explicit finite element modelling method for masonry walls under out-of-plane loading. *Eng. Struct.* 113, 103–120. doi:10.1016/j.engstruct.2016.01.026

Page, A. W. (1995). "Unreinforced masonry structures: an Australian overview," in Pacific Conference on Earthquake Engineering (PCEE) (Melbourne, Australia).

Parisi, F., and Augenti, N. (2013). Assessment of unreinforced masonry cross sections under eccentric compression accounting for strain softening. *Constr. Build. Mater.* 41, 654–664. doi:10.1016/j.conbuildmat.2012.12.039

Park, D., Kim, S., Jin, S., Choi, Y., Kim, H., and Hong, J. W. (2025). Seismic vulnerability assessment of leaning U-shaped masonry fence walls. *Earthq. Spectra* 41, 2177–2202. doi:10.1177/87552930251320413

Peduto, D., Nicodemo, G., Maccabiani, J., Ferlisi, S., D'Angelo, R., and Marchese, A. (2016). Investigating the behaviour of buildings with different foundation types on soft soils: two case studies in the Netherlands. *Procedia Eng.* 158, 529–534. doi:10.1016/j.proeng.2016.08.484

Peduto, D., Ferlisi, S., Nicodemo, G., Reale, D., Pisciotta, G., and Gullà, G. (2017). Empirical fragility and vulnerability curves for buildings exposed to slow-moving landslides at medium and large scales. *Landslides* 14, 1993–2007. doi:10.1007/s10346-017-0826-7

Peduto, D., Korff, M., Nicodemo, G., Marchese, A., and Ferlisi, S. (2019). Empirical fragility curves for settlement-affected buildings: analysis of different intensity parameters for seven hundred masonry buildings in the Netherlands. *Soils Found.* 59, 380–397. doi:10.1016/j.sandf.2018.12.009

Penner, O., and Elwood, K. J. (2016a). Out-of-Plane dynamic stability of unreinforced masonry walls in one-way bending: parametric study and assessment guidelines. *Earthq. Spectra* 32, 1699–1723. doi:10.1193/011715EQS011M

Penner, O., and Elwood, K. J. (2016b). Out-of-Plane dynamic stability of unreinforced masonry walls in one-way bending: shake table testing. *Earthq. Spectra* 32, 1675–1697. doi:10.1193/011415EQS009M

Pesci, A., Teza, G., Loddo, F., Rossetti, A., Gambuzzi, I., and Gambuzzi, A. (2024). The role of remote sensing to enlarge knowledge on health state of a historical building hit by earthquake: the case of garisenda leaning tower (bologna). *Ann. Geophys.* 67, S550. doi:10.4401/ag-9119

Prosperi, A. (2025). *Modelling of subsidence induced damage to masonry buildings: influence of soil heterogeneity on settlement and development of fragility*. Delft, Netherlands: Delft University of Technology.

Prosperi, A., Korswagen, P. A., Korff, M., Schipper, R., and Rots, J. G. (2023a). Empirical fragility and ROC curves for masonry buildings subjected to settlements. *J. Build. Eng.* 68, 106094. doi:10.1016/j.jobe.2023.106094

Prosperi, A., Longo, M., Korswagen, P. A., Korff, M., and Rots, J. G. (2023b). "Accurate and efficient 2D modelling of historical masonry buildings subjected to settlements in comparison to 3D approaches," in International Conference on Structural Analysis of Historical Constructions (Kyoto, Japan).

Prosperi, A., Longo, M., Korswagen, P. A., Korff, M., and Rots, J. G. (2023c). Sensitivity modelling with objective damage assessment of unreinforced masonry façades undergoing different subsidence settlement patterns. *Eng. Struct.* 286, 116113. doi:10.1016/j.engstruct.2023.116113

Prosperi, A., Longo, M., Korswagen, P. A., Korff, M., and Rots, J. G. (2024). 2D and 3D modelling strategies to reproduce the response of historical masonry buildings subjected to settlements. *Int. J. Archit. Herit.* 19, 1–17. doi:10.1080/15583058.2024.2325472

RLP Tourismus website (2025). *RLP tourismus website*. Available online at: https://www.rlp-tourismus.com/en/ (Accessed September 10, 2025).

Robazza, B. R., Brzev, S., Yang, T. Y., Elwood, K. J., Anderson, D. L., and Mcewen, B. (2018). Out-of-Plane behavior of slender reinforced masonry shear walls under In-Plane loading. *Exp. Investig.* 144, 1–16. doi:10.1061/(ASCE)ST.1943-541X.0001968

Rots, J. G., Messali, F., Esposito, R., Jafari, S., and Mariani, V. (2016). "Thematic keynote computational modelling of masonry with a view to Groningen induced seismicity," in 10th International Conference on Structural Analysis of Historical Constructions (Leuven, Belgium).

Sajid, H. U., Ashraf, M., Ali, Q., and Sajid, S. H. (2018). Effects of vertical stresses and flanges on seismic behavior of unreinforced brick masonry. *Eng. Struct.* 155, 394–409. doi:10.1016/j.engstruct.2017.11.013

Selby, R. G., and Vecchio, F. J. (1993). *Three-dimensional constitutive relations for reinforced concrete*. Toronto, Ontario, Canada: University of Toronto.

Sharma, S., Tomassetti, U., Grottoli, L., and Graziotti, F. (2020). Two-way bending experimental response of URM walls subjected to combined horizontal and vertical seismic excitation. *Eng. Struct.* 219, 110537. doi:10.1016/j.engstruct.2020.110537

Sorrentino, L., D'Ayala, D., de Felice, G., Griffith, M. C., Lagomarsino, S., and Magenes, G. (2016). Review of out-of-plane seismic assessment techniques applied to existing masonry buildings. *Int. J. Archit. Herit.* 11, 1–20. doi:10.1080/15583058.2016.1237586

Standards New Zealand (2004). *NZS 4230:2004, design of reinforced concrete masonry structures*. Wellington, New Zealand.

Taucer, F., and Pinto Vieira, A. (2007). *Eur 22868 EN: field manual for post-earthquake damage and safety assessment and short term countermeasures (AeDES)*.

University of Auckland (2011). *NZSEE: assessment and improvement of unreinforced masonry buildings for earthquake resistance, New Zealand society of earthquake engineering, supplement to "assessment and improvement of the structural performance of buildings in earthquakes*. Auckland, New Zealand.

van Ginkel, J., Ruigrok, E., Stafleu, J., and Herber, R. (2022). Development of a seismic site-response zonation map for the Netherlands. *Nat. Hazards Earth Syst. Sci.* 22, 41–63. doi:10.5194/nhess-22-41-2022

Vanin, F., Penna, A., and Beyer, K. (2020). A three-dimensional macroelement for modelling the in-plane and out-of-plane response of masonry walls. *Earthq. Eng. Struct. Dyn.* 49, 1365–1387. doi:10.1002/eqe.3277